The FASEB Journal article fj.13-238725. Published online November 7, 2013.

Spare mitochondrial respiratory capacity permits human adipocytes to maintain ATP homeostasis under hypoglycemic conditions

Michaela Keuper,[*,1,2] Martin Jastroch,[†,‡,1] Chun-Xia Yi,[†,‡] Pamela Fischer-Posovszky,[§] Martin Wabitsch,[§] Matthias H. Tschöp,[†,‡] and Susanna M. Hofmann*

*Institute for Diabetes and Regeneration Research and [†]Institute for Diabetes and Obesity, Helmholtz Zentrum München, German Research Center for Environmental Health, Neuherberg, Germany; [‡]Technische Universität München, Munich, Germany; and [§]Division of Pediatric Endocrinology and Diabetes, Department of Pediatrics and Adolescent Medicine, Ulm University Medical Center, Ulm, Germany

ABSTRACT **Mitochondrial dysfunction in white adipose tissue plays a key role in the pathogenesis of type 2 diabetes. Emerging evidence specifically suggests that altered oxidative phosphorylation in adipocytes may have a relevant effect on systemic glucose homeostasis, requiring understanding of adipocyte bioenergetics. We analyzed energetic flux of an intact human adipocyte cell model by plate-based respirometry and extracellular acidification. During differentiation, we discovered that glycolytic ATP production was increasingly replaced by mitochondrial oxidative metabolism (from 20 to 60%). This observation was corroborated by simultaneous up-regulation of canonical mitochondrial gene programs, such as peroxisome proliferator-activated receptor γ coactivator α (PGC1α; 150-fold) and cytochrome c-1 (CytC; 3-fold). Mimicking diabetic phenotypes by exposure to various glucose levels (0, 5, and 25 mM) resulted in immediate adjustments of glycolytic and mitochondrial activity that aimed to maintain intracellular ATP. We conclude that ATP deficits by mitochondrial failure are compensated by glycolytic ATP production, resulting in inefficient conversion of glucose to cellular ATP. Metabolic inefficiency may enhance glucose uptake, therefore improving systemic glucose homeostasis. Notably, mature adipocytes developed a high spare respiratory capacity (increased by 6-fold) permitting rapid adaptation to metabolic changes. Spare respiratory capacity may also allow additional metabolic scope for energy dissipation, potentially offering new therapeutic targets for the treatment of metabolic disease.—Keuper, M., Jastroch, M., Yi, C.-X., Fischer-Posovszky, P., Wabitsch, M., Tschöp, M. H., Hofmann, S. M. Spare mitochondrial respiratory capacity permits human adipocytes to maintain ATP homeostasis under hypoglycemic conditions. *FASEB J.* 28, 000–000 (2014). www.fasebj.org**

Key Words: glycolysis · lactate secretion · oxidative phosphorylation · hyperglycemic

OBESITY IS THE MOST PREVALENT cause for chronic diseases such as type 2 diabetes mellitus, hypertension, and cancer. Increased fat mass leads to dysfunctional properties in adipocytes, which have been causally linked to metabolic disease (1). Although mitochondrial dysfunction in various tissues has been associated with obesity and has been widely accepted as a central cause for insulin resistance and its complications (2), white adipose tissue mitochondrial function has been overlooked in the past, mostly due to the low mitochondrial content in adipocytes.

Recent evidence revealed that mitochondria increase in number (3) and undergo mitochondrial remodeling during white adipocyte differentiation (4, 5), pointing to an important, although underappreciated role of white fat cell mitochondria in adipogenesis. Although mitochondria content is significantly lower in white adipocytes as compared with brown adipocytes or muscle cells, a recent mitochondria protein compendium study detected more diverse variety of protein in white fat as compared with heart, muscle, or brain mitochondria (6), pointing toward potentially unknown and

Abbreviations: ATP, adenosine triphosphate; CytC, cytochrome c-1; 2DG, 2-deoxy-glucose; ECAR, extracellular acidification rate; ETC, electron transport chain; FCCP, carbonyl cyanide-4-(trifluoromethoxy)phenylhydrazone; HPRT, hypoxanthine-guanine phosphoribosyltransferase; OCR, oxygen consumption rate; oxphos, oxidative phosphorylation; PGC1α, peroxisome proliferator-activated receptor γ coactivator α; PPARγ, peroxisome proliferator-activated receptor γ; PPR, proton production rate; SGBS, Simpson-Golabi-Behmel syndrome

[1] These authors contributed equally to this work.

[2] Correspondence: Helmholtz Zentrum München, German Research Center for Environmental Health (GmbH), Institute for Diabetes and Regeneration Research, Ingolstaedter Landstr. 1, 85764 Neuherberg, Germany. E-mail: michaela.keuper@helmholtz-muenchen.de

doi: 10.1096/fj.13-238725

unique functions of white fat mitochondria. The traditional view, that white fat mitochondria play a minor role in the development of metabolic disease, has been further challenged by the recent findings that mitochondrial content is reduced in white adipose tissue of obese rodents and humans (7, 8), in conjunction with compromised oxygen consumption on isoproterenol stimulation in isolated white adipose tissue from obese patients (9). Most notably, there is emerging evidence that modulating mitochondrial function in white fat tissue may affect adipocyte energy metabolism and presumably whole-body energy homeostasis: adipocyte-specific overexpression of MitoNEET, an outer mitochondrial membrane protein, in leptin-deficient mice decreases mitochondrial oxygen consumption rates in association with an improvement in glucose intolerance and hepatic insulin sensitivity (10). In contrast, similar systemic effects on glucose tolerance have been achieved by increasing mitochondrial respiration through the fat tissue-specific deletion of the mitochondrial transcription factor A (TFAM; ref. 11). It is likely that in both cases mitochondrial adenosine triphosphate (ATP) production is compromised and potentially leads to a compensatory increase in glycolytic ATP production that may ultimately result in increased glucose uptake and benefits for systemic glucose homeostasis. These findings emphasized the importance of white adipose tissue mitochondria as an attractive drug target, but there is still little knowledge about their control of energy metabolism and homeostasis. The assessment of how glucose levels modulate energy metabolism and substrate utilization in adipocytes will assist in understanding and potentially treating metabolic abnormalities. The characterization of oxidative phosphorylation (oxphos) and its interplay with glycolysis is technically challenging. Recent advances in technologies using real-time analysis of oxygen consumption and extracellular acidification rates in undisturbed, adherent cell culture models may be utilized to address these questions.

Herein we established measurements of energetic flux using plate-based respirometry (mitochondrial oxidation) and acidification rates (glycolysis) in intact human white adipocytes of the Simpson-Golabi-Behmel syndrome (SGBS) cell strain, thus allowing full assessment of the bioenergetic status of the fat cell. This cell strain, originally derived from a patient with the SGBS, possesses a high capacity for *in vitro* differentiation into adipocytes (12) and has been demonstrated to function like primary isolated human preadipocytes and adipocytes (13). To better understand the mechanisms of oxphos for the maintenance of cellular ATP, we further divided cellular respiration into mitochondrial and nonmitochondrial, and evaluated mitochondrial respiration in ATP turnover/synthesis, proton leak, and maximal substrate oxidation using specific pharmacological inhibitors. We also characterized the relative contribution of mitochondrial respiration to energy homeostasis during fat cell differentiation. Finally, to determine whether diabetic conditions affect glycolysis and oxphos rates we used this system to compare bioenergetics of preadipocytes and adipocytes under hypo- and hyperglycemic conditions.

MATERIALS AND METHODS

Materials

Cell culture media and supplements were from Invitrogen (Darmstadt, Germany). All other chemicals and reagents were obtained from Sigma-Aldrich (München, Germany) if not otherwise stated.

Experimental system

SGBS cells were grown as reported previously (12, 14) in DMEM/F12 (1:1) containing 33 μM biotin, 17 μM pantothenate, and antibiotics (basal medium) plus 10% FCS. For respiratory analysis, cells were seeded on XF96-PS plates (Seahorse Bioscience, North Billerica, MA, USA) for RNA analysis, cells were seeded on 12-well-plates; and for the lactate assay, cells were seeded on 96-well-plates. At 90% confluency, cells were either analyzed as preadipocytes (d 0) or adipogenic differentiation was induced as reported previously (12, 13). Briefly, cells were washed 2 times with PBS and cultured in basal medium supplemented with 10 μg/ml iron-poor transferrin, 20 nM insulin, 200 pM triiodothyronine, 100 nM cortisol, 2 μM rosiglitazone (BRL 49653; Caymen Chemicals, Ann Arbor, MI, USA), 250 μM isobutylmethylxanthine (IBMX), and 25 nM dexamethasone for 4 d. After 4 d, cells were cultured in basal medium supplemented with 10 μg/ml iron-poor transferrin, 20 nM insulin, 200 pM triiodothyronine, and 100 nM cortisol. Cells were analyzed as adipocytes 10 d (d 10) after induction of differentiation.

Determination of cell number and rate of adipogenic differentiation

The total cell number, the number of preadipocytes, and the number of adipocytes were estimated in the monolayers by direct counting using a net micrometer (Leica, Wetzlar, Germany). Cells were counted as adipocytes, when >5 lipid droplets were visible in the cell. The rate of adipogenic differentiation is the percentage of adipocytes of the total number. Images were obtained using a Di-Li 2028 inverse microscope equipped with a 5-Mpx USB camera (Distelkamp Electronics, Kaiserslautern, Germany).

Confocal microscopy

SGBS cells were grown on Nunc-Lab-Tek chambered coverglasses (Fisher Scientific, Schwerte, Germany) and stained either at d 0 or at d 10 after induction of differentiation with 40 nM MitoTracker Green (Life Technologies, Darmstadt, Germany) for 30 min at 37°C. Then, cells were washed and observed by confocal microscopy (Leica SP5).

Expression of mitochondria-related genes

RNA was harvested using the RNeasy lipid tissue kit (Qiagen, Hilden, Germany). After reverse transcription (SuperScript; Invitrogen), expression of peroxisome proliferator-activated receptor γ (PPARγ), PPARγ coactivator α (PGC1α), and cytochrome c-1 (CytC) was analyzed using real-time PCR (Lightcycler; Roche, Grenzach, Germany) together with the house-

keeping gene hypoxanthine-guanine phosphoribosyltransferase (HPRT). Sequences of specific primers are as follows: PPARγ-fw: 5′-GATCCAGTGGTTGCAGATTACAA-3′; PPARγ-rev: 5′-GAGGGAGTTGGAAGGCTCTTC-3′; PGC1α-fw: 5′-CTCAAATATCTGACCACAAACGATGACCCTC-3′; PGC1α-rev: 5′-GTTGTTGGTTTGGCTTGTAAGTGTTGTGAC-3′; CytC-fw: 5′-TGTGCTACACGGAGGATGAAGCTAAGGA-3′; CytC-rev: 5′-TAGTCCTCACCACCATGCCTAGCTC-3′; HPRT-fw: 5′-GAGATGGGAGGCCATCACATTGTAGCCCTC-3′; and HPRT-rev: 5′-CTCCACCAATTACTTTTATGTCCCCTGTTGACTGGTC-3′.

Energetic pathway studies

Preadipocytes and adipocytes were washed with XF assay medium containing 0, 5, or 25 mM glucose (pH adjusted to 7.5) and incubated for 1 h in a 37°C air incubator with these glucose concentrations. The XF96 plate (Seahorse Bioscience) was then transferred to a temperature controlled (37°C) Seahorse (extracellular flux) analyzer (Seahorse Bioscience) and subjected to an equilibration period. One assay cycle comprised a 1-min mix, 2-min wait, and 3-min measure period. After 4 basal assay cycles, oligomycin (1 μg/ml) was added by automatic pneumatic injection to inhibit the ATP synthase and thus approximate the proportion of respiration used to drive ATP synthesis. After 3 further assay cycles, carbonyl cyanide-4-(trifluoromethoxy)phenylhydrazone (FCCP; 0.5 μM) was added the same way to stimulate maximal respiration in mitochondria by uncoupling ATP synthesis from electron transport. After another 3 assay cycles, rotenone (4 μM) plus antimycin A (2 μM) was added to determine the nonmitochondrial respiratory rate, which was subtracted from all other rates. Oxygen consumption rate (OCR) traces and a scheme about the different modules that we analyzed are depicted in **Fig. 2*A***. Coupling efficiency was calculated as the oligomycin-sensitive fraction of mitochondrial respiratory activity. ATP production from oxphos was calculated using a phosphate/oxygen (P/O) ratio of 2.3 (15).To determine extracellular acidification rates (ECARs) derived from glycolysis, measurements were ended by addition of 2-deoxy-glucose (2DG; 100 mM). ECAR traces and the different modules that we analyzed are depicted in **Fig. 3*A***. ECARs were converted into proton production rates (PPRs) by taking into account the buffer capacity. 2DG-sensitive PPR estimates ATP production from glycolysis with a 1:1 ratio.

Lactate assay

Preadipocytes and adipocytes were incubated in fresh medium (same as for the Seahorse measurements) supplemented with or without oligomycin (1 μg/ml). After 3 h, concentration of lactate in the supernatant was determined using the Lactate Assay Kit (BioVision, Heidelberg, Germany) according to the manufacturer's manual.

Statistics

If not stated otherwise in the figure legends, the data presented are the means ± SEM of 9 independently performed experiments. Each experiment compromises data of 4–8 wells/group. For statistical comparison, 1-way ANOVA (*post hoc*: Holm-Sidak) was performed**.** PGC1a mRNA expression data failed to meet the assumption of normal distribution and were thus analyzed with ANOVA on ranks (*post hoc*: Tukey). Values of $P < 0.05$ were considered statistically significant. All statistical tests were performed using SigmaStat 12.0 (Systat Software, San Jose, CA, USA).

RESULTS

Adipocyte differentiation induces expression of mitochondrial markers and alterations of the mitochondrial network

To monitor changes in cellular respiration during adipogenesis, SGBS preadipocytes were seeded on XF96 plates, and differentiation was induced. Cells were analyzed as preadipocytes (d 0), as well as at d 10 after induction of *in vitro* differentiation into adipocytes. The degree of differentiation was monitored by light microscopy (exemplified in **Fig. 1*A***), assessing the number of lipid-laden adipocytes. While lipids were absent at d 0, the counting of differentiated adipocytes at d 10 resulted in 73 ± 3% differentiation rate (Fig. 1*B*). While the ratio of preadipocytes and adipocytes differed between d 0 and 10, the total cell number per analyzed well was the same (d0: 1394±49 cells/well; d10: 1391±37 cells/well; Fig. 1*C*). The morphological assessment of adipocyte differentiation was supported by increased gene expression of PPARγ, an important transcription factor promoting adipogenesis and a broadly accepted adipocyte marker (Fig. 1*D*). Furthermore, the expression levels of the mitochondrial gene regulator PGC1α (Fig. 1*E*) and CytC, an essential component of the mitochondrial respiratory chain (Fig. 1*F*), were significantly elevated in differentiated adipocytes as compared with preadipocytes, demonstrating that human SGBS cells increase their mitochondrial content during adipogenesis. Of note, when we stained preadipocytes and adipocytes with MitoTracker Green and studied mitochondria by confocal live imaging, we detected pronounced differences in the mitochondrial network (Fig. 1*G*). In preadipocytes, we observed a long reticulum of mitochondria (Fig. 1*Ga*), whereas at d10 of adipogenic differentiation this network and reticular mitochondria disappeared (Fig. 1*Gc*). Mitochondria were diffuse, and the network structure was no longer visible around growing lipid droplets, shown here in an early stage of differentiation (Fig. 1*Gb*, red asterisks).

Increased cellular respiration during adipogenesis is caused by mitochondrial and nonmitochondrial fluxes

OCRs of adherent preadipocytes and differentiated adipocyte cultures were measured using a Seahorse XF96 extracellular flux analyzer. Cellular respiration was increased 4-fold in differentiated adipocytes as compared with preadipocytes, suggesting markedly increased mitochondrial activity (Fig. 2*A*, *B*).

To determine processes that consume oxygen in adipocytes, specific mitochondrial inhibitors were sequentially added to the cells. Figure 2*A* shows the time-lapse measurements of OCR in absolute values, which can be partitioned into distinct modules of oxygen consumption reporting different mitochondrial and cellular processes (Fig. 2*A*, right panel). At the end

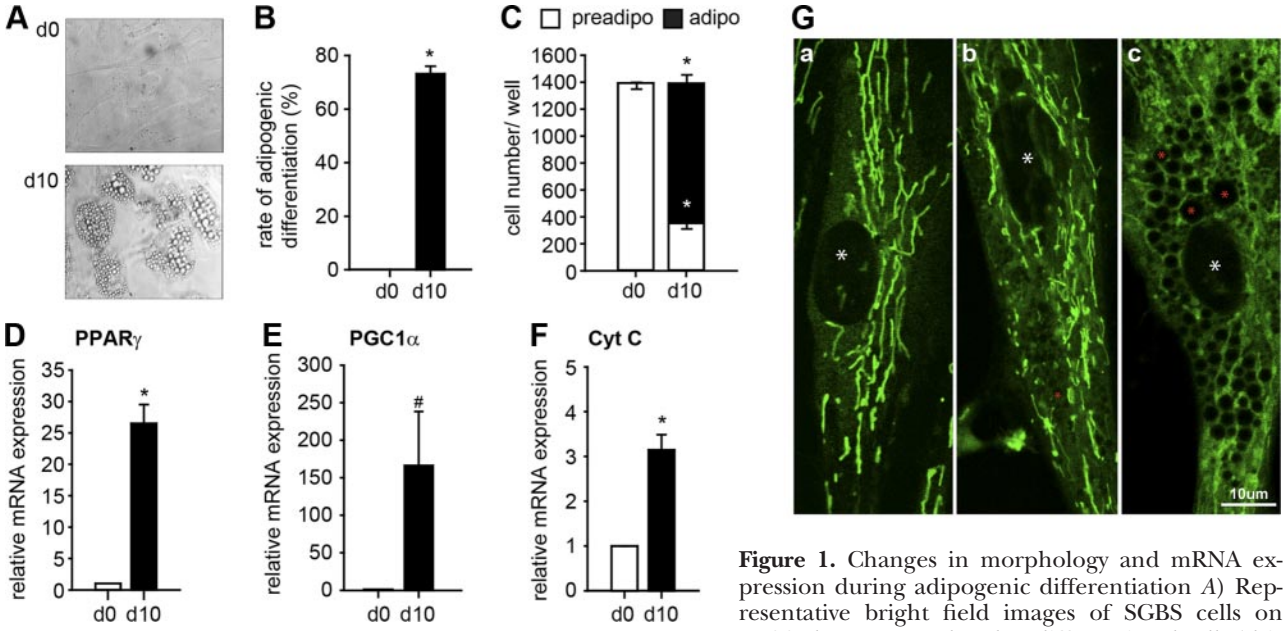

Figure 1. Changes in morphology and mRNA expression during adipogenic differentiation *A*) Representative bright field images of SGBS cells on XF96 plates. We analyzed undifferentiated cells (d 0, preadipocytes) and cells 10 d (d 10, adipocytes) after induction of differentiation. Pictures were taken shortly before the Seahorse measurement. *B*) Rate of adipogenic differentiation was determined. Data are means ± SEM of 32–37 wells on 9 independent XF96 plates. $*P < 0.001$ *C*) Number of adherent preadipocytes and adipocytes was determined. Data are means ± SEM of 32–37 wells on 9 independent XF96 plates. $*P < 0.001$. *D–F*) mRNA expression of PPARγ (*D*), PGC1α (*E*), and CytC (*F*) was analyzed by qPCR. Results were normalized to the expression of HPRT ($2^{-\Delta Ct}$ method) and related to preadipocytes (d 0; $2^{-\Delta\Delta Ct}$ method). Data are means ± SEM of 3 (PPARγ and CytC) or 8 (PGC1α) independent experiments. $^{\#}P < 0.05$; $*P < 0.001$. *G*) SGBS preadipocytes and adipocytes were labeled with MitoTracker Green. *a*) Preadipocytes. *b*) Early stage of differentiation. *c*) Late stage of differentiation (adipocyte d 10). White asterisks indicate the nucleus; red asterisks indicate lipid droplets. One representative cell is shown.

of the experiment, complete inhibition of mitochondrial flux by addition of rotenone (complex I inhibitor) and antimycin A (complex III inhibitor) allowed distinction between mitochondrial and nonmitochondrial respiration (Fig. 2*B*).

Basal mitochondrial respiration was increased in differentiated adipocytes, suggesting higher ATP turnover and demand (Fig. 2*C*). When corrected for oxygen consumption driving the mitochondrial proton leak (inhibiting ATP synthase with oligomycin; Fig. 2*C*), the resulting ATP-linked respiration that reports ATP turnover (ATP synthesis equals consumption) was significantly higher in differentiated adipocytes as compared with undifferentiated cells (Fig. 2*C*).

The maximal ATP output of mitochondria is controlled by substrate oxidation capacity, which was determined by inducing maximal substrate oxidation (addition of the protonophore FCCP). Figure 2*D* shows that maximal substrate oxidation was higher in differentiated adipocytes as compared with preadipocytes. Spare respiratory capacity was increased in differentiated adipocytes and was determined by subtracting basal respiration from FCCP-induced respiration (Fig. 2*D*). While preadipocytes possessed almost no mitochondrial reserve capacity (2.3±0.8 pmol O_2/min), adipocytes showed unused capacity of mitochondrial function (11.0±2.0 pmol O_2/min), which may allow metabolic scope. Taken together, the higher cellular respiration of adipocytes can be attributed to both, mitochondrial and nonmitochondrial respiration.

Mitochondrial (coupling) efficiency does not change during adipogenic differentiation

The increase of proton leak respiration in mature adipocytes as compared with preadipocytes (Fig. 2*C*) may be interpreted as decreased efficiency caused by higher proton permeability over the mitochondrial inner membrane but may also just be a result of increased substrate oxidation capacity (16). Mitochondrial efficiency, termed coupling efficiency (CE; ref. 17), calculates the proportion of nutrient energy that is converted into ATP while the rest is lost as heat. Calculating CE from the ratio of ATP-linked and proton leak respiration, we found no significant difference of CE between preadipocytes and differentiated adipocytes (0.54±0.10 and 0.65±0.02, respectively; Fig. 2*E*).

Glycolytic activity, measured as extracellular acidification rates, decreases during adipogenic differentiation

Glycolysis, contributing 2 ATP molecules per oxidized glucose, represents an ATP source complementary to mitochondria. Glycolysis was approximated by ECAR of preadipocytes and adipocytes, simultaneously to OCR (Fig. 3*A*). With the use of specific inhibitors, ECARs were used to characterize glycolysis (Fig. 3*A*, right panel). Preadipocytes showed higher cellular acidification values as compared with adipocytes (Fig. 3*B*). By addition of 2DG, an inhibitor of glycolysis, ECAR values

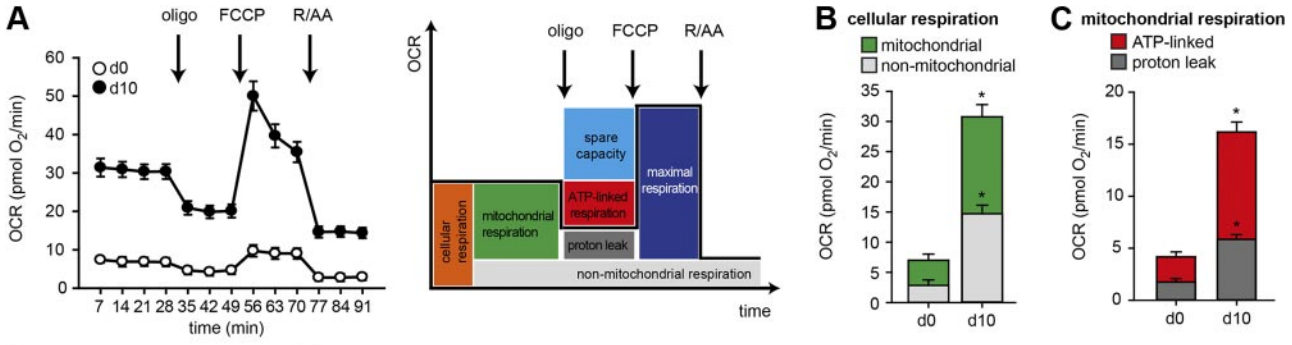

Figure 2. Adipocytes show a higher mitochondrial activity. Cellular respiration and respiration after interference of mitochondrial pathways with specific inhibitors was analyzed using a XF96 extracellular flux analyzer as described in Materials and Methods. Cultures of SGBS preadipocytes (d 0) and adipocytes (d 10) were used. *A*) Left panel: OCR over time. Right panel: scheme showing dissection of the oxygen consuming processes of a cell. *B*) Cellular respiration was dissected into mitochondrial (green) and nonmitochondrial (gray) respiration using the ETC inhibitors rotenone (R; 4 μM, R) and antimycin A (AA; 2 μM). *C*) Mitochondrial respiration was further dissected into proton leak (dark gray) and ATP-linked respiration (red) using the ATP-synthase inhibitor oligomycin (oligo; 1 μg/ml). *D*) Maximal respiration (dark blue) of preadipocytes and adipocytes can be obtained after addition of a chemical uncoupler (FCCP, 0.5 μM) and by subtracting the nonmitochondrial respiration rates. The portion of spare respiratory capacity (light blue) was obtained by subtracting basal respiration from maximal respiration rates. *E*) Mitochondrial coupling efficiencies were calculated as the fraction of mitochondrial oxygen consumption that is sensitive to oligomycin, reflecting the fraction used to drive ATP synthesis. AU, arbitrary units. All data are means ± SEM of 9 independent experiments. $*P < 0.001$.

were corrected for nonglycolytic acidification. While nonglycolytic acidification rates of preadipocytes and adipocytes were not significantly different (3.8±0.8 *vs.* 2.8±0.5 mpH/min; Fig. 3*B*), basal glycolytic rates were higher in preadipocytes (Fig. 3*B*). The difference in basal glycolytic ECARs in preadipocytes as compared with adipocytes demonstrated higher glycolytic ATP production in preadipocytes. The relation of ECARs reporting glycolysis was alternatively consolidated by addition of oxamate (inhibiting the conversion of pyruvate to lactate), instead of 2DG (data not shown). Inducing maximal glycolytic rates by inhibiting mitochondrial ATP production with oligomycin further supported the trend toward higher glycolytic capacity in preadipocytes (Fig. 3*C*).

Lactate secretion rates decrease during adipogenic differentiation

ECAR, measured with Seahorse technology, may be affected by tricarboxylic acid cycle (TCA) activity and carbon dioxide release, the latter being converted to bicarbonate, thus contributing to extracellular acidification. As secreted lactate levels are an alternative measure of anaerobic glycolysis, unaffected by TCA cycle by-products, we analyzed lactate concentrations in the medium supernatant of preadipocytes and adipocytes. We found that preadipocytes secrete more lactate than adipocytes (33.2±6.4 *vs.* 13.6±2.2 pmol/min) under basal conditions (Fig. 3*D*), verifying the higher glycolytic activity in preadipocytes as compared with adipocytes (Fig. 3*B*). Furthermore, induction of lactate secretion by oligomycin elucidated maximal glycolytic rates, supporting significant differences between preadipocytes and mature adipocytes (Fig. 3*E*).

ATP demand of preadipocytes and differentiated adipocytes is mainly fueled by glycolysis

ATP homeostasis is essential for cell survival and function. Therefore, we next estimated ATP fluxes from the XF96 data as described in Materials and Methods, distinguishing between oxphos and glycolysis.

The calculation of the flux data demonstrated that the mitochondrial ATP output in adipocytes was higher as compared with preadipocytes (**Fig. 4*A***). In contrast, glycolytic ATP production was not significantly different but tended to be lower in differentiated adipocytes (Fig. 4*B*). Notably, the total ATP turnover did not change significantly during adipogenesis (preadipocytes: 73.9±9.9 pmol ATP/min; adipocytes: 92.5±9.2 pmol ATP/min; Fig. 4*C*). Calculating the proportion of ATP production from oxphos and glycolysis demonstrated that preadipocytes fueled their ATP demand mainly by glycolytic processes (Fig. 4*D*), while adipocytes increased the proportion of mitochondrial ATP (preadipocytes: 18.0±4.2% *vs.* adipocytes: 56.5± 6.8%). There was, however, still a high contribution (43.5%) of glycolytic ATP.

Preadipocytes demonstrate a compensatory increase in ATP-linked respiration in the absence of glucose

In the next step, we asked how cellular energetics are balanced in response to different physiological and

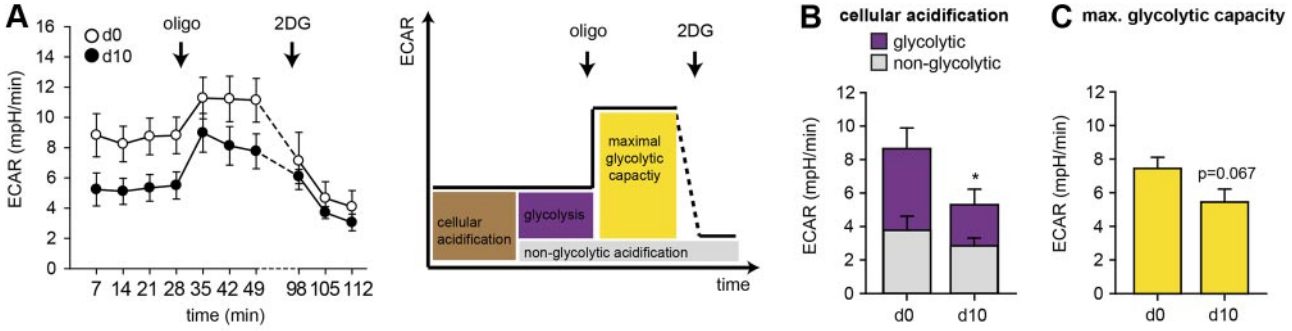

Figure 3. ECAR decreases during adipogenesis. *A*) Left panel: ECAR was recorded simultaneously with OCR of preadipocytes (d 0) and adipocytes (d 10) over time with a Seahorse XF96 extracellular flux analyzer, as described in Materials and Methods. Right panel: cellular ECAR can be further dissected into different modules as depicted. Data after FCCP and rotenone/antimycin A injection were not used for ECAR analysis and are depicted as dashed lines. *B*) By inhibiting glycolysis with 2DG (100 mM) as the last step in the measurements, cellular acidification was broken down to nonglycolytic acidification (gray) and acidification due to glycolysis (purple). *C*) By inhibiting mitochondrial ATP synthesis with oligomycin, the maximal glycolytic capacity was obtained. *D*) Basal lactate secretion from preadipocytes (d 0) and adipocytes (d 10) was analyzed as described in Materials and Methods. *E*) Lactate secretion of preadipocytes and adipocytes treated with 1 μg/ml oligomycin. In *A–C*, data are means ± SEM of 9 independent experiments. In *D* and *E*, data are means ± SEM of 3 independently stimulated wells measured in triplicates and mathematically adjusted to cell number present in XF96 well. $*P < 0.001$.

pathophysiological levels of glucose supply. Therefore, we challenged the fat cell system with hypoglycemic (0 mM glucose) and hyperglycemic (25 mM glucose) conditions, comparing the results for preadipocytes and adipocytes to a physiologically "normal" glucose concentration of 5 mM (Figs. 2 and 3).

Analyzing cellular respiration in preadipocytes, we detected increased basal respiration at 0 mM glucose (10.5±1.2 pmol O_2/min, n=10) as compared with 5 mM glucose (7.0±1.0 pmol O_2/min; n=9) and 25 mM glucose (7.5±0.8 pmol O_2/min; n=11). By dissecting the cellular respiration as described above, higher cellular respiration at 0 mM glucose was attributable to an increase in ATP-linked respiration only (**Fig. 5*A***) resulting in a higher mitochondrial ATP production (Fig. 5*B*). Nonmitochondrial respiration (0 mM glucose: 3.4±1.0 pmol O_2/min; 5 mM glucose: 2.8±0.9 pmol O_2/min; 25 mM glucose: 3.3±0.4 pmol O_2/min) and proton leak respiration (0 mM glucose: 2.1±0.4 pmol O_2/min; 5 mM glucose: 1.7±0.3 pmol O_2/min; 25 mM glucose: 1.5±0.3 pmol O_2/min) were not significantly different. Furthermore, we detected neither a significant difference in coupling efficiency nor in maximal substrate oxidation of the preadipocytes (data not shown). ATP production from glycolysis was decreased in preadipocytes under hypoglycemic conditions (Fig. 5*C*). Thus, preadipocytes compensated this decreased glycolytic ATP production by an increase in ATP-linked respiration (Fig. 5*A*), increasing the proportion of mitochondrial ATP production (Fig. 5*B*). Calculated total ATP production, however, decreased to ~40 pmol ATP/min when preadipocytes were exposed to hypoglycemic conditions (Fig. 5*D*). This strong decrease in ATP homeostasis under hypoglycemic conditions (Fig. 5*D*) suggests that ATP demand under normal conditions (5mM glucose) cannot be

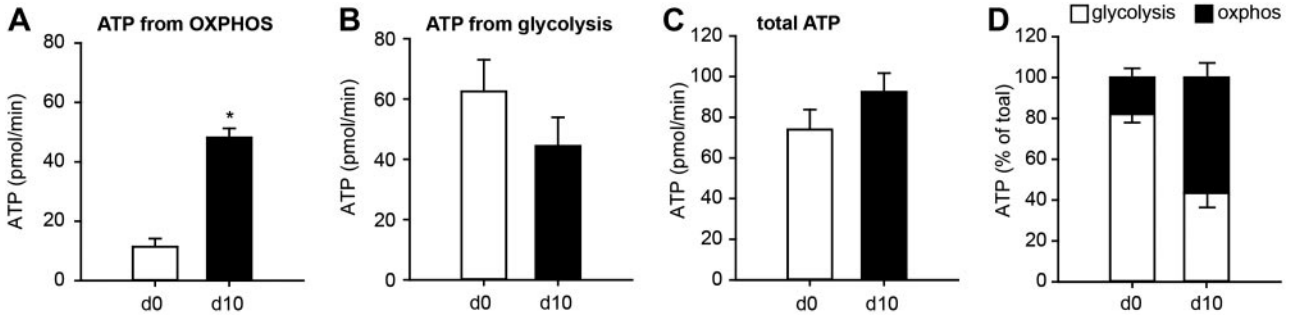

Figure 4. Preadipocytes and adipocytes show a bias for glycolytic ATP production. Calculations were performed as described in Materials and Methods. *A*) ATP production rates of oxphos pathways. *B*) ATP production rates of glycolysis, as estimated *via* PPR. *C*) Sum of ATP produced by oxphos and glycolysis. *D*) Percentage of oxphos (solid bar) and glycolytic (open bar) ATP production on total ATP production. All data are means ± SEM of 9 independent experiments. $*P < 0.001$.

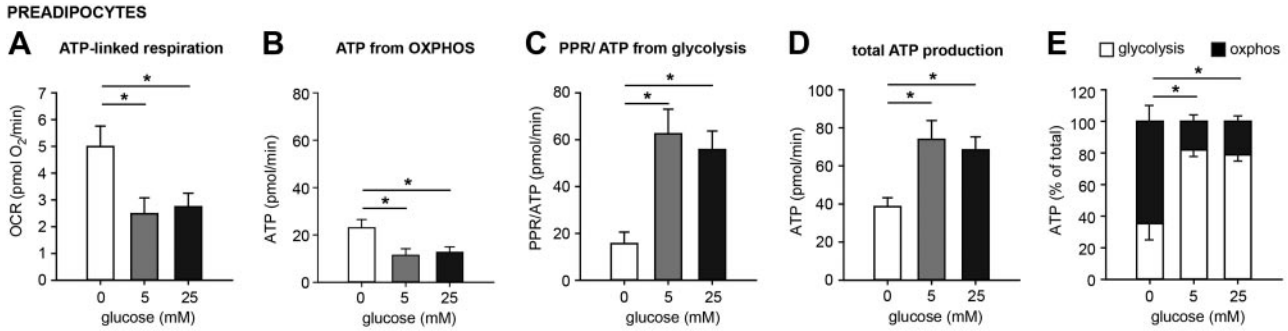

Figure 5. Preadipocytes increase ATP-linked respiration under hypoglycemic conditions. Respiration and acidification rates were recorded for preadipocytes treated with 0, 5, or 25 mM glucose and detailed dissection/analysis was performed as described above for Figs. 2–4. *A*) ATP-linked respiration of preadipocytes under hypoglycemic (0 mM glucose), normoglycemic (5 mM glucose), and hyperglycemic (25 mM glucose) conditions. *B*) Mitochondrial ATP production obtained by converting ATP-linked respiration. *C*) PPR/ATP production from glycolysis. *D*) Sum of ATP produced by oxphos and glycolysis. *E*) Percentage of oxphos (solid bar) and glycolytic (open bar) ATP production on total ATP production. All data are means ± SEM of $n = 10$ (0 mM), $n = 9$ (5 mM), and $n = 11$ (25 mM) independent experiments. $^*P < 0.001$.

fully compensated by mitochondrial ATP production (accounting for ~65% of the total produced ATP; Fig. 5*E*).

Adipocytes switch from mitochondrial ATP production toward glycolytic ATP production with increasing glucose concentrations

Next, we analyzed the bioenergetic profile of mature, lipid-laden adipocytes under hypo- and hyperglycemic conditions**.** Adipocytes showed a significantly lower ATP-linked respiration under hyperglycemic conditions as compared with hypoglycemic conditions (**Fig. 6*A***), which can be translated in significantly lower oxidative ATP production (Fig. 6*B*). In parallel, ATP production of glycolysis was higher with 25 mM glucose as compared with 0 mM glucose (Fig. 6*C*). The calculated total ATP production revealed no significant differences, suggesting no effects of glucose on ATP homeostasis (0 mM glucose: 71.2±7.2 pmol ATP/min; 5 mM glucose: 92.4±9.2 pmol ATP/min; 25 mM glucose: 82.8±7.7 pmol ATP/min; Fig. 6*D*) Furthermore, oxphos and glycolysis appeared interchangeable. Adipocytes decreased the proportion of mitochondrial ATP when glucose was present (Fig. 6*E*), suggesting that adipocytes switch on mitochondrial ATP production only when glycolysis is not sufficient to fulfill ATP demand. Notably, although glucose levels modulate ATP production, ATP-linked respiration is always higher in adipocytes as compared with preadipocytes (**Fig. 7*A, B***).

DISCUSSION

In the present study, we established concurrent measurements of aerobic and glycolytic energetic pathways of human white fat cells in real time, showing for the first time the close link of these two pathways in human white fat cells. We detected differences in both pathways in preadipocytes and adipocytes, with adipocytes using more aerobic processes whereas preadipocytes depended almost exclusively on glycolytic energy production. Modulating the extracellular environment

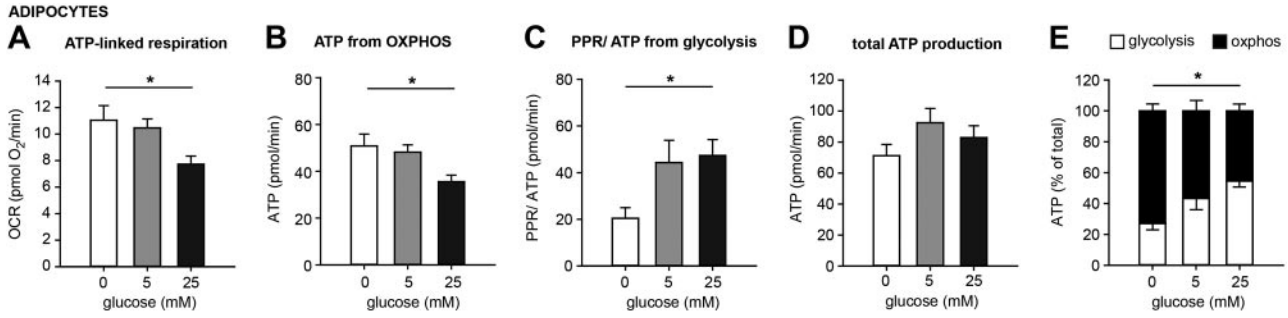

Figure 6. Adipocytes shift their ATP production from oxphos toward glycolytic pathways with increasing glucose concentrations. Respiration and acidification rates were recorded for adipocytes treated with 0, 5, or 25 mM glucose, and detailed dissection/analysis was performed as described above for Figs. 2–4. *A*) ATP-linked respiration of adipocytes under hypoglycemic (0 mM glucose), normoglycemic (5 mM glucose), and hyperglycemic (25 mM glucose) conditions. *B*) Mitochondrial ATP production obtained by converting ATP-linked respiration. *C*) PPR/ATP production from glycolysis. *D*) Sum of ATP produced by oxphos and glycolysis. *E*) Percentage of oxphos (solid bar) and glycolytic (open bar) ATP production on total ATP production. All data are means ± SEM of $n = 10$ (0 mM), $n = 9$ (5 mM), and $n = 11$ (25 mM) independent experiments. $^*P < 0.001$.

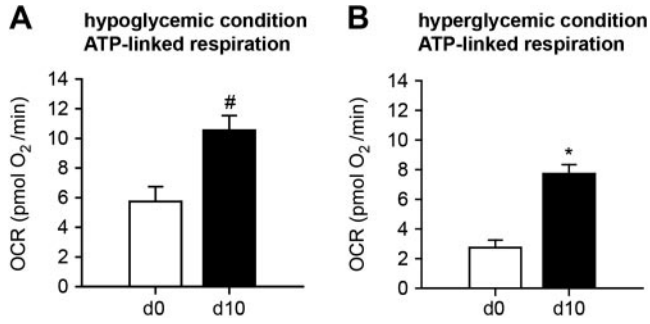

Figure 7. Adipocytes (*vs.* preadipocytes) show higher ATP-linked respiration under hypo- and hyperglycemic conditions. *A*) Comparison of ATP-linked respiration between preadipocytes (d 0) and adipocytes (d 10) under hypoglycemic conditions (0 mm glucose). *B*) Comparison of ATP-linked respiration between preadipocytes (d 0) and adipocytes (d 10) under hyperglycemic conditions (25 mm glucose). All data are means + SEM of $n = 10$ (0 mM) and $n = 11$ (25 mM) independent experiments. $^{*}P < 0.001$; $^{\#}P < 0.003$.

(glucose concentration), we showed that preadipocytes are not able to fully compensate for a loss in glycolytic ATP production by increasing their mitochondrial ATP production. Surprisingly, glycolysis also seemed to be the preferred energy-producing pathway in adipocytes, since they were turning down mitochondrial ATP production as soon as more glucose was available. However, mitochondria in adipocytes were able to react and compensate for the loss of glycolytic ATP production, thereby allowing metabolic scope.

We applied calculations to convert both glycolysis and ATP-linked respiration to ATP production, based on the well-defined stoichiometry of ATP production (15). Our results revealed important features in adipocytes bioenergetics: ATP demand/turnover does not change during differentiation; glycolytic ATP production was replaced by mitochondrial ATP production during differentiation under normal glucose concentrations; to maintain ATP homeostasis, glycolytic ATP and mitochondrial ATP were interchangeable; and energy homeostasis in adipocytes was controlled by cellular ATP turnover not by nutrient supply, as found *e.g.*, for pancreatic β cells (17). This is an important finding that requires consideration for drug targeting. To improve metabolic disease, currently the therapeutic scope would be to increase energy combustion. For that it is mandatory to either increase ATP turnover or dissipate mitochondrial proton motive force.

We further showed that mitochondrial respiration increased during differentiation, which is caused by increase in substrate oxidation capacity. The increase of substrate oxidation allowed higher mitochondrial ATP output, which was reflected in higher ATP-linked respiration. Importantly, unused respiratory capacity increased ~6-fold during differentiation, which can be used during physiological challenge and stress. While this spare capacity is used in neuronal cells to match fluctuating ATP demands (18), the physiological importance of spare capacity is less defined in adipocytes and could be targeted for energy dissipation without disturbance of cellular ATP homeostasis. In perspective, spare mitochondrial capacity may represent an attractive therapeutic target to dissipate energy or rebalance adipocyte metabolism during metabolic disorders.

Due to our normalization to cell number and not to protein content, the mitochondria-dependent metabolic scope seen in human SGBS adipocytes might be due to changes in mitochondrial density in each cell. Similarly, murine 3T3-L1 cells increase the amount of mitochondria per cell, showing up to a 30-fold increase in several mitochondrial proteins during adipogenic differentiation, which may profoundly affect cellular respiration (19). We found increased expression of mitochondrial biogenesis-related gene PGC1α and CytC, the latter a component of the electron transport chain (ETC) in mitochondria, suggesting that human SGBS cells similar to murine 3T3-L1 cells increased their mitochondrial content during adipogenesis. Characterizing the mitochondrial network in human preadipocytes and adipocytes with confocal live imaging, we found profound differences (Fig. 1*G*): In preadipocytes, mitochondria were visible as a long reticulum that gradually disappears during differentiation. In mature fat cells mitochondria were more evenly distributed around lipid droplets with no visible network structure. Dynamic processes such as fission and fusion are implicated in this remodeling process (20). This is in line with two very recent reports on murine fat cells during adipogenesis suggesting that mitochondria undergo structural changes and that fission and fusion are crucial to adipogenesis (4, 5). Taking into account our findings regarding functional changes of whole cell bioenergetics during adipogenesis, we hypothesize that mitochondria undergo a complex transformation possibly consisting of structural, content and functional changes. In view of the importance of white adipose tissue mitochondria as an attractive drug target against the metabolic syndrome (10, 11), these preliminary findings warrant further investigation to understand the underlying mechanisms that can be then exploited for drug development.

Our results in human adipocytes herein confirmed earlier evidence for higher cellular respiration in murine 3T3-L1 adipocytes as compared with 3T3-L1 preadipocytes (21). However, previously this higher cellular respiration was not further dissected into the different cellular oxygen consuming processes such as mitochondrial and nonmitochondrial respiration. With the use of a Clark-type electrode, maximal respiration induced by FCCP was neither detected in mature rat adipocytes (22) nor increased during adipogenesis in 3T3-L1 adipocytes (4). In this study, we clearly detected a higher FCCP respiration in human adipocytes as compared with preadipocytes. Higher rates of ATP-linked respiration (coupled) as well as uncoupled (oligomycin) respiration in mature human adipocytes can be explained by an increase in maximal substrate oxidation and not uncoupled respiration as coupling effi-

ciencies also did not change. These contradictory results maybe due to different adipocyte cell types, culture conditions, or measurement techniques in which we assume advantage of plate-based respirometry with undisturbed adherent cell culture. Our data showing between 45 and 73% contribution of oxphos to total ATP production depending on glucose availability are in line with measurements obtained by microcalorimetry. With microcalorimetry, the authors showed that 68% of total energy production originates from oxidative pathways in human primary adipocytes (23), suggesting that the bioenergetic profile of human SGBS adipocytes closely resembles human primary adipocytes.

We showed that the contribution of glycolysis to ATP generation decreased during differentiation and was replaced by mitochondrial ATP production. As mitochondrial and glycolytic ATP production appeared mutually exchangeable to maintain ATP homeostasis, anaerobic glycolysis was able to replace mitochondrial ATP production and restore ATP homeostasis, as it may happen during mitochondrial dysfunction. This concept provides a rational explanation for recent discoveries demonstrating that mitochondrial dysfunction improves systemic glucose homeostasis, presumably shifting metabolism toward glycolysis (10, 11). The shift toward glycolysis would decrease the ATP yield ~15-fold, assuming that lactate is cleared from the system. Notably, it has been demonstrated that hypoxic conditions increase lactate secretion of adipocytes (24), which strongly supports our ATP homeostasis model: when oxygen for mitochondrial ATP production is rate-limiting, fat cells increase their glycolytic ATP production to fuel ATP demand, resulting in increased lactate secretion. Elevated plasma lactate levels have been reported in patients with diabetes and determined to be a risk factor for diabetes (25, 26). Furthermore, lactate secretion from adipose tissue of obese patient is increased (27).

We showed that the proportion of nonmitochondrial respiration to cellular respiration was high and further increased during adipogenesis (preadipocytes 28%, adipocytes 47%). Enzymes such as oxidases located at the endoplasmic reticulum (ER), may be responsible for increased oxygen consumption, as well as increased oxidative folding reactions at the ER that are a general hallmark of endocrine (secretory) cells (28). Since adipocytes are very active endocrine cells (29), the increased nonmitochondrial respiration may reflect the enhanced secretory function of fat cells.

Although anaerobic glycolysis decreased during differentiation, we still found considerable glycolytic rates at d 10 of differentiation, indicating that glycolytic ATP production may be preferred. In particular at a high concentration of glucose, the adipocytes shifted from oxidative metabolism to glycolytic ATP production (Fig. 6*E*). A possible explanation can be attributed to metabolites for *de novo* lipogenesis that derive from glycolysis (30), *e.g.*, dihydroxyacetone phosphate as a precursor for the glycerol backbone of triacylglycerides (31).

Disrupting either mitochondrial function or glycolysis diverts metabolite fluxes, *e.g.*, long-term mitochondrial uncoupling reduces triglyceride accumulation by redirecting carbon flux away from fatty acid synthesis toward lactate production (32).

Herein we focused on the regulation of glycolysis and oxphos in adipocytes by glucose. Besides nutrients like glucose, hormones such as insulin and adrenaline modulate glucose and lipid metabolism in adipocytes *in vivo*. These modulating elements are yet missing in the present study and require further extensive studies to address how they affect glycolysis and oxphos. However, the comprehensive analysis of cellular energy metabolism in adipocytes presented in this study will assist to identify molecular players that promote changes seen in obesity, thereby offering novel drug targets to restore dysfunctional properties. FJ

This work was funded (in part) by the Helmholtz Alliance ICEMED (Imaging and Curing Environmental Metabolic Diseases) through the Initiative and Network Fund of the Helmholtz Association. The authors declare no conflicts of interest.

REFERENCES

1. Guilherme, A., Virbasius, J. V., Puri, V., and Czech, M. P. (2008) Adipocyte dysfunctions linking obesity to insulin resistance and type 2 diabetes. *Nat. Rev. Mol. Cell Biol.* **9,** 367–377
2. Kim, J., Wei, Y., and Sowers, J. R. (2008) Role of mitochondrial dysfunction in insulin resistance. *Circ. Res.* **102,** 401–414
3. Wilson-Fritch, L., Burkart, A., Bell, G., Mendelson, K., Leszyk, J., Nicoloro, S., Czech, M., and Corvera, S. (2003) Mitochondrial biogenesis and remodeling during adipogenesis and in response to the insulin sensitizer rosiglitazone. *Mol. Cell. Biol.* **23,** 1085–1094
4. Ducluzeau, P.-H., Priou, M., Weitheimer, M., Flamment, M., Duluc, L., Iacobazi, F., Soleti, R., Simard, G., Durand, A., Rieusset, J., Andriantsitohaina, R., and Malthièry, Y. (2011) Dynamic regulation of mitochondrial network and oxidative functions during 3T3-L1 fat cell differentiation. *J. Physiol. Biochem.* **67,** 285–296
5. Kita, T., Nishida, H., Shibata, H., Niimi, S., Higuti, T., and Arakaki, N. (2009) Possible role of mitochondrial remodelling on cellular triacylglycerol accumulation. *J. Biochem. (Tokyo)* **146,** 787–796
6. Pagliarini, D. J., Calvo, S. E., Chang, B., Sheth, S. A., Vafai, S. B., Ong, S.-E., Walford, G. A., Sugiana, C., Boneh, A., Chen, W. K., Hill, D. E., Vidal, M., Evans, J. G., Thorburn, D. R., Carr, S. A., and Mootha, V. K. (2008) A mitochondrial protein compendium elucidates complex I disease biology. *Cell* **134,** 112–123
7. Choo, H.-J., Kim, J.-H., Kwon, O.-B., Lee, C. S., Mun, J. Y., Han, S. S., Yoon, Y.-S., Yoon, G., Choi, K.-M., and Ko, Y.-G. (2006) Mitochondria are impaired in the adipocytes of type 2 diabetic mice. *Diabetologia* **49,** 784–791
8. Wilson-Fritch, L., Nicoloro, S., Chouinard, M., Lazar, M. A., Chui, P. C., Leszyk, J., Straubhaar, J., Czech, M. P., and Corvera, S. (2004) Mitochondrial remodeling in adipose tissue associated with obesity and treatment with rosiglitazone. *J. Clin. Invest.* **114,** 1281–1289
9. Yehuda-Shnaidman, E., Buehrer, B., Pi, J., Kumar, N., and Collins, S. (2010) Acute stimulation of white adipocyte respiration by PKA-induced lipolysis. *Diabetes* **59,** 2474–2483
10. Kusminski, C. M., Holland, W. L., Sun, K., Park, J., Spurgin, S. B., Lin, Y., Askew, G. R., Simcox, J. A., McClain, D. A., Li, C., Askew, G. R., Simcox, J. A., McClain, D. A., Li, C., and Scherer,

P. E. (2012) MitoNEET-driven alterations in adipocyte mitochondrial activity reveal a crucial adaptive process that preserves insulin sensitivity in obesity. *Nat. Med.* **18,** 1539–1549
11. Vernochet, C., Mourier, A., Bezy, O., Macotela, Y., Boucher, J., Rardin, M. J., An, D., Lee, K. Y., Ilkayeva, O. R., Zingaretti, C. M., Emanuelli, B., Smyth, G., Cinti, S., Newgard, C. B., Gibson, B. W., Larsson, N. G., and Kahn, C. R. (2012) Adipose-specific deletion of TFAM increases mitochondrial oxidation and protects mice against obesity and insulin resistance. *Cell Metab.* **16,** 765–776
12. Wabitsch, M., Brenner, R. E., Melzner, I., Braun, M., Möller, P., Heinze, E., Debatin, K. M., and Hauner, H. (2001) Characterization of a human preadipocyte cell strain with high capacity for adipose differentiation. *Int. J. Obes. Relat. Metab. Disord.* **25,** 8–15
13. Fischer-Posovszky, P., Newell, F. S., Wabitsch, M., and Tornqvist, H. E. (2008) Human SGBS cells–a unique tool for studies of human fat cell biology. *Obes. Facts* **1,** 184–189
14. Keuper, M., Dzyakanchuk, A., Amrein, K. E., Wabitsch, M., and Fischer-Posovszky, P. (2011) THP-1 macrophages and SGBS adipocytes–a new human in vitro model system of inflamed adipose tissue. *Front. Syst. Transl. Endocrinol.* **2,** 89
15. Brand, M. D. (2005) The efficiency and plasticity of mitochondrial energy transduction. *Biochem. Soc. Trans.* **33,** 897–904
16. Jastroch, M., Hirschberg, V., and Klingenspor, M. (2012) Functional characterization of UCP1 in mammalian HEK293 cells excludes mitochondrial uncoupling artefacts and reveals no contribution to basal proton leak. *Biochim. Biophys. Acta* **1817,** 1660–1670
17. Affourtit, C., Jastroch, M., and Brand, M. D. (2011) Uncoupling protein-2 attenuates glucose-stimulated insulin secretion in INS-1E insulinoma cells by lowering mitochondrial reactive oxygen species. *Free Radic. Biol. Med.* **50,** 609–616
18. Nicholls, D. G. (2009) Spare respiratory capacity, oxidative stress and excitotoxicity. *Biochem. Soc. Trans.* **37,** 1385
19. Newton, B. W., Cologna, S. M., Moya, C., Russell, D. H., Russell, W. K., and Jayaraman, A. (2011) Proteomic analysis of 3T3-L1 adipocyte mitochondria during differentiation and enlargement. *J. Proteome Res.* **10,** 4692–4702
20. Youle, R. J., and Bliek, A. M. van der (2012). Mitochondrial fission, fusion, and stress. *Science* **337,** 1062–1065
21. Von Heimburg, D., Hemmrich, K., Zachariah, S., Staiger, H., and Pallua, N. (2005) Oxygen consumption in undifferentiated versus differentiated adipogenic mesenchymal precursor cells. *Respir. Physiol. Neurobiol.* **146,** 107–116
22. Wang, T., Si, Y., Shirihai, O. S., Si, H., Schultz, V., Corkey, R. F., Hu, L., Deeney, J. T., Guo, W., and Corkey, B. E. (2010) Respiration in adipocytes is inhibited by reactive oxygen species. *Obesity (Silver Spring)* **18,** 1493–1502
23. Böttcher, H., and Fürst, P. (1996) Microcalorimetric and biochemical investigations of thermogenesis and metabolic pathways in human white adipocytes. *Int. J. Obes. Relat. Metab. Disord.* **20,** 874–881
24. Pérez de Heredia, F., Wood, I., and Trayhurn, P. (2010) Hypoxia stimulates lactate release and modulates monocarboxylate transporter (MCT1, MCT2, and MCT4) expression in human adipocytes. *Pflügers Arch.* **459,** 509–518
25. Crawford, S. O., Hoogeveen, R. C., Brancati, F. L., Astor, B. C., Ballantyne, C. M., Schmidt, M. I., and Young, J. H. (2010) Association of blood lactate with type 2 diabetes: the Atherosclerosis Risk in Communities Carotid MRI Study. *Int. J. Epidemiol.* **39,** 1647–1655
26. Juraschek, S. P., Shantha, G. P. S., Chu, A. Y., Miller, E. R., Guallar, E., Hoogeveen, R. C., Ballantyne, C. M., Brancati, F. L., Schmidt, M. I., Pankow, J. S., and Young, J. H. (2013) Lactate and risk of incident diabetes in a case-cohort of the Atherosclerosis Risk in Communities (ARIC) Study. *PLoS One* **8,** e55113
27. Qvisth, V., Hagström-Toft, E., Moberg, E., Sjöberg, S., and Bolinder, J. (2007) Lactate release from adipose tissue and skeletal muscle in vivo: defective insulin regulation in insulin-resistant obese women. *Am. J. Physiol. Endocrinol. Metab.* **292,** E709–E714
28. Tu, B. P., and Weissman, J. S. (2002) The FAD- and O2-dependent reaction cycle of Ero1-mediated oxidative protein folding in the endoplasmic reticulum. *Mol. Cell* **10,** 983–994
29. Kershaw, E. E., and Flier, J. S. (2004) Adipose tissue as an endocrine organ. *J. Clin. Endocrinol. Metab.* **89,** 2548–2556
30. Guo, X., Li, H., Xu, H., Woo, S., Dong, H., Lu, F., Lange, A. J., and Wu, C. (2012) Glycolysis in the control of blood glucose homeostasis. *Acta Pharm. Sin. B* **2,** 358–367
31. Collins, J. M., Neville, M. J., Pinnick, K. E., Hodson, L., Ruyter, B., van Dijk, T. H., Reijngoud, D.-J., Fielding, M. D., and Frayn, K. N. (2011) De novo lipogenesis in the differentiating human adipocyte can provide all fatty acids necessary for maturation. *J. Lipid Res.* **52,** 1683–1692
32. Si, Y., Shi, H., and Lee, K. (2009) Metabolic flux analysis of mitochondrial uncoupling in 3T3-L1 adipocytes. *PLoS One* **4,** e7000

Received for publication July 19, 2013.
Accepted for publication October 24, 2013.